Mon. Not. R. Astron. Soc. **000**, 1–12 (2011) Printed 14 January 2013 (MN LaTeX style file v2.2)

arXiv:1103.1692v1 [astro-ph.CO] 9 Mar 2011

Large scale nested stellar discs in NGC 7217*

Olga K. Sil'chenko[1,2]*, Igor V. Chilingarian[3,1], Natalia Ya. Sotnikova[4,5]†,
Victor L. Afanasiev[6]
[1] *Sternberg Astronomical Institute, Moscow State University, 13 Universitetski prospect, 119992, Moscow, Russia*
[2] *Isaac Newton Institute of Chile, Moscow Branch*
[3] *Centre de Données astronomiques de Strasbourg – Observatoire de Strasbourg, CNRS UMR 7550,*
Université de Strasbourg, 11 Rue de l'Université, 67000 Strasbourg, France
[4] *St.Petersburg State University, Russia*
[5] *Isaac Newton Institute of Chile, St. Petersburg Branch*
[6] *Special Astrophysical Observatory, Russian Academy of Sciences, Nizhnij Arkhyz, Russia*

Accepted 2011 March 7. Received 2011 March 2; in original form 2010 November 4

ABSTRACT

NGC 7217 is an unbarred early-type spiral galaxy having a multi-segment exponential light profile and a system of starforming rings of the unknown origin; it also possesses a circumnuclear gaseous polar disc. We analysed new long slit spectroscopic data for NGC 7217 and derived the radial distributions of its stellar population parameters and stellar and gaseous kinematics up to the radius of $r \approx 100''$ ($\sim$ 8 kpc). We performed the dynamical analysis of the galaxy by recovering its velocity ellipsoid at different radii, and estimated the scaleheights of its two exponential discs. The inner exponential stellar disc of NGC 7217 appears to be thin and harbours intermediate age stars ($t_{\mathrm{SSP}} \approx 5$ Gyr). The outer stellar disc seen between the radii of 4 and 7 kpc is very thick ($z_0 = 1 \ldots 3$ kpc), metal-poor, [Fe/H]< -0.4 dex, and has predominantly young stars, $t_{SSP} = 2$ Gyr. The remnants of minor mergers of gas-rich satellites with an early-type giant disc galaxy available in the GalMer database well resemble different structural components of NGC 7217, suggesting two minor merger events in the past responsible for the formation of the inner polar gaseous disc and large outer starforming ring. Another possibility to form the outer ring is the re-accretion of the tidal streams created by the first minor merger.

Key words: galaxies: evolution – galaxies: structure – spiral galaxies – individual: NGC 7217.

1 INTRODUCTION

Currently, our views on galaxy structure are changing dramatically. The classical view that every disc galaxy represents a combination of a de-Vaucouleurs' bulge, a sort of an elliptical galaxy inside a larger stellar system, and an exponential large scale stellar disc (e.g. Freeman 1970) does not conform to modern high accuracy observations, in particular to photometric data. With the surface photometry reaching low surface brightness limits, down to 27–28 mag arcsec^{-2} in the r-band, the brightness profiles of most large scale stellar discs cannot be fitted by a single component exponential law: 90 per cent of discs turn to be either truncated or antitruncated (Pohlen & Trujillo 2006). Bulges also appear to be far from de-Vaucouleurs' spheroids: when approximated by a Sersic law with a free power parameter, they show surface brightness profile shapes spanning a range of n, with the mean $n \approx 2$ (Andredakis et al. 1995; Seigar & James 1998; Graham 2001; Mollenhoff & Heidt 2001). Some morphological types, namely, spirals later than Sbc (Andredakis & Sanders 1994) and lenticulars (Balcells et al. 2003; Laurikainen et al. 2005), exhibit exponential surface brightness profiles for their bulges. The scatter in the concentration parameter n is thought to be related to variety of bulge formation mechanisms; a range of scenarios restricts also dynamical properties of the bulges of different types.

Currently, all bulges are divided into two categories, "classical" high luminosity bulges which are suggested to be formed by fast violent events like mergers, and "pseudobulges". The bulges of the latter type promulgated by J. Kormendy (see Kormendy 1993 and earlier conference contributions), are thought to form by secular evolution from the gaseous and stellar material of the disc (Kormendy & Kennicutt 2004), in particular through the

---

* Based on the observations with the Russian 6m telescope
† E-mail: nsot-astro@mail.ru (NYS); olga@sai.msu.su (OKS)

© 2011 RAS

central disc heating by bars (Combes & Sanders 1981), hence they have to resemble discs by some of their dynamical characteristics. Balcells et al. (2007) noted a presence of a lot of separate discy stellar structures in the centers of spiral galaxies, and Erwin et al. (2003) demonstrated that sometimes inner discs in early-type disc galaxies might resemble bulges. Although, following this fashion, a great variety of central structures often found in early-type disc galaxies (see e.g. Erwin & Sparke 2002) is now treated as the pseudobulges including nuclear discs and bars (Drory & Fisher 2007), we would like to stay on the classical point of view that the principal difference between discs and bulges is related to their thickness: discs are thin, flat, roughly two-dimensional structures, and bulges must be thick and three-dimensional by definition. Pseudobulges being produced by secular-evolution mechanisms may have exponential surface brightness profiles (Friedli & Benz 1995), but they differ principally from the exponential stellar discs by their thickness. To put a quantitative criterion to distinguish between discs and spheroids, let us take a look on the phenomenology. E. Hubble classified elliptical galaxies by their shape ranged between *E0* (the axis ratio of 1) and *E7* (the axis ratio of 3); however many former *E7* galaxies are now thought to be lenticulars, NGC 3115 being a famous example. As for the large-scale stellar discs, the closest axis ratio to the transition towards spheroids is perhaps demonstrated by the thick disc of the edge-on spiral galaxy NGC 891: its ratio of the exponential scalelength to the exponential scaleheight is about 3.3 (Ibata et al. 2009). Hence, we consider that the ratio of scalelength to scaleheight of about 3 is a reasonable frontier between spheroids and discs.

While analysing a photometric structure of a disc galaxy inclined to the line of sight, we can trace the ellipticity of its isophotes to establish a transition radius where the thick central structure, the bulge, delegates a dominance to the thin disc: it is the radius where the isophote ellipticity stops raising. For a galaxy at a small inclination, it is very difficult to distinguish between its exponential pseudobulge and a disc without a 3D dynamical model of a galaxy. We attempted to construct such a model for the galaxy NGC 7217, for which there is still no agreement on the structure and origin of its inner subsystems.

NGC 7217 is a giant early-type spiral galaxy seen almost face-on. The distance to the galaxy adopted in our paper, 18.4 Mpc, was estimated from the Tully–Fisher relation by Russell (2002). It corresponds to the spatial scale of 0.08 kpc arcsec^{-1}. NGC 7217 is listed in the catalogue of isolated galaxies by Karachentseva (1973); in a more recent study by Bettoni et al. (2001), the density of its environment is also estimated as zero. The galaxy whose evolution is supposedly free of the environmental influence, demonstrates a set of enigmatic structures which can be best explained by (a set of) minor mergers. First of all, it has three starforming rings, at radii of 11, 33, and 75 arcsec (Buta & Crocker 1993) looking like resonance structures requiring the presence of a non-axisymmetric potential (Verdes-Montenegro et al. 1995), while the galaxy itself is unbarred. Buta et al. (1995) proposed to decompose the whole galaxy into a small disc and a large mildly triaxial deVaucouleurs spheroid dominating at all distances from the center. The dominance of the bulge triaxial potential over the whole galaxy caused the formation of three resonance rings with high density gas concentration and ongoing star formation. Later we undertook our own decomposition of the NGC 7217 structure and have found the two large exponential components with different scalelengths[1], 12.5 arcsec, or 1 kpc for the inner one and 35.8 arcsec, or about 3 kpc for the outer one (Sil'chenko & Afanasiev 2000). The inner component has larger intrinsic ellipticity than the outer one and so may be oval providing the necessary triaxiality of the potential to put the rings at the resonance radii. The bulge, if any, is small, confined within the innermost (nuclear) ring, and exponential. To choose between the alternate ways of decomposition, the kinematical data and a dynamical model are needed. The situation is complicated by the fresh (?) remnants of a minor merger presented by counterrotating stars in the inner disc (Merrifield & Kuijken 1994) and the inner gas polar disc within $R \approx 4$ arcsec (Sil'chenko & Afanasiev 2000).

In this paper we present the results of long slit spectroscopy of NGC 7217. Our goal is the diagnostics of the nature of the two large scale exponential structures in this galaxy. The inner exponential structure may be an inner disc (a thin structure) or a pseudobulge (a thick structure). Since NGC 7217 is seen nearly face-on, the isophote ellipticity is a poor indicator of the stellar component thickness as it is close to zero over the whole galaxy. But with the stellar velocity dispersion profiles along the major and minor axes we can try to estimate the scaleheights of the stellar components from dynamical considerations. In Section 2 we describe our observations, data reduction and analysis, in Section 3 we provide our new estimates of the stellar population properties at different radii. The principal Section 4 gives our dynamical consideration of the NGC 7217 large scale structures, and Section 5 contains a discussion about the origin of the galaxy structure including the comparison with numerical simulations. In Section 6 we give a brief summary of our results.

2 OBSERVATIONS AND DATA REDUCTION.

The spectroscopic observations were carried out with the SCORPIO[2] universal spectrograph (Afanasiev & Moiseev 2005) installed at the prime focus of the Russian 6-m Bol'shoy Teleskop Azimutal'nyy (BTA) operated by the Special Astrophysical Observatory, Russian Academy of Sciences. We used the VPHG2300G grating providing an intermediate spectral resolution ($R \approx 2200$) in a relatively narrow wavelength region ($4800 < \lambda < 5500$ Å) however containing a rich set of strong absorption line features making it suitable for studying both internal kinematics and stellar populations of a galaxy. The chosen spectral range also includes several emission lines, Hβ, [O III], and [N I], which we used to derive the gas kinematics and line ratios. The slit was 1.0 arcsec wide and 6 arcmin long. The 2k×2k EEV CCD42-40 detector used in the 1×2 binning mode provided a spectral sampling of 0.37 Å pix^{-1} and a spatial scale of 0.357 arcsec pix^{-1}.

---

[1] The bulge also demonstrates an exponential profile with a scalelength ∼ 4 arcsec (Sil'chenko & Afanasiev 2000).

[2] For a description of the SCORPIO instrument, see `http://www.sao.ru/hq/moisav/scorpio/scorpio.html`

We observed NGC 7217 in two slit positions going through the centre, along minor and major axes of its inner isophotes. The major axis spectrum, P.A.=81 deg, was obtained on 6/Oct/2008 with an integration time of 80 min under atmosphere conditions with good transparency and intermediate image quality of $1.7''$ FWHM corresponding to the median seeing at the telescope site. The minor axis data at P.A.=169 deg were collected during two nights October, 6, 2008 and October, 8, 2008 with a total exposure time of 75 min under bad variable transparency and seeing quality of ~ 3 arcsec making them notably shallower than the major axis spectra. We obtained the following calibrations: night time internal flat field and arc line spectra, the GD 248 spectrophotometric standard star, and high signal-to-noise twilight spectral frames.

Data reduction and analysis for the spectral data of NGC 7217 was identical to that of the lenticular galaxy NGC 6340 presented in Chilingarian et al. (2009). We refer to that paper for all details, here we give only essential information required for understanding our data analysis and interpretation.

The primary data reduction steps included bias subtraction, flat fielding and cosmic ray hit removal using the Laplacian filtering technique (van Dokkum 2001). Then, we built the wavelength solution by identifying arc lines and fitting their positions using a 3rd order two-dimensional polynomial along and across dispersion, and linearised the spectra. The obtained wavelength solution had fitting residuals of about 0.08 Å RMS.

The SCORPIO spectrograph has significant variations of the spectral line-spread-function (LSF) along and across the wavelength direction (see Moiseev 2008 and Chilingarian et al. 2009 for details). In our observations of NGC 7217, we used the peripheral regions of the slit beyond 2 arcmin from the galaxy centre to estimate the night sky spectrum, therefore it was very important to take the LSF variations into account in order to minimize the effects of the sky subtraction artefacts on the data analysis. We mapped the LSF by fitting the high-resolution ($R = 10000$) Solar spectrum against the twilight spectra at 64 positions along the slit in five slightly overlapping wavelength segments covering the spectral range of the SCORPIO setup with the penalized pixel fitting technique (Cappellari & Emsellem 2004). We used the Gauss-Hermite parametrization up to the 4th order (van der Marel & Franx 1993) to represent the LSF shape.

Then, we modelled the night sky spectrum at every position along the slit following the procedure described in detail in Chilingarian et al. (2009) where the main step was the parametric signal recovery applied to the sky spectrum taken in the outer regions of the slit in the Fourier space as follows:

$$f(x,\lambda) = F^{-1}(F(f(\mathrm{sky},\lambda))\frac{F(\mathcal{L}(x))}{F(\mathcal{L}(\mathrm{sky}))}), \qquad (1)$$

where $f(x,\lambda)$ denotes a sky spectrum at the position x along the slit with its parametrized LSF $\mathcal{L}(x)$; $f(\mathrm{sky},\lambda)$ is the night sky spectrum in any region of the slit with the LSF $\mathcal{L}(\mathrm{sky})$, and F, F^{-1} are the direct and inverse Fourier transforms respectively. The night sky model created in this fashion results in a nearly Poisson quality of the sky subtraction which is absolutely crucial for our analysis of the external regions of the galaxy.

3 STELLAR POPULATIONS AND INTERNAL KINEMATICS OF NGC 7217

We derived the parameters of internal kinematics and stellar populations of NGC 7217 by fitting high-resolution PEGASE.HR (Le Borgne et al. 2004) simple stellar population (SSP) models against our spectra with the NBursts full spectral fitting technique (Chilingarian et al. 2007b,a). The SSP models were computed using the Salpeter (1955) stellar initial mass function. The fitting algorithm is picking up a template from a grid of stellar population models in the age–metallicity space convolved with the instrumental response of the spectrograph (see previous section), broadening it with the line-of-sight velocity distribution (LOSVD) of a galaxy represented by the Gauss-Hermite parametrization up to the 4th order, i.e. v, σ, h_3, and h_4. The models are multiplied pixel by pixel by the n^{th} order Legendre polynomial continuum which is used to account for possible imperfections of the flux calibration and for the internal dust extinction in a galaxy. All kinematical and stellar population parameters are determined in a single non-linear minimization loop therefore reducing possible degeneracies. The χ^2 is penalized towards purely Gaussian LOSVD as explained in Cappellari & Emsellem (2004) in order to stabilise the solution in case of low signal-to-noise ratios and/or insufficient spectral sampling of the data. We stress that for the dynamical analysis presented below, we use the pure Gaussian LOSVD parametrization without χ^2 penalization.

The PEGASE.HR models are constructed from empirical stellar spectra in the Solar neighbourhood where the value of α-element abundances is known to correlate with the overall metallicity. Therefore, at intermediate and high metallicities, our SSP models are representative of the solar α/Fe abundance ratio. However, Chilingarian et al. (2008) showed that supersolar α/Fe ratios bias neither age nor metallicity estimates when using the NBursts spectral fitting technique, and Sil'chenko & Afanasiev (2000) found nearly solar α/Fe in NGC 7217.

NGC 7217 possesses quite strong emission lines in its spectrum especially in the regions corresponding to the rings with ongoing star formation. Therefore we had to exclude from the fitting procedure several narrow 20 Å–wide regions around emission lines (Hβ $\lambda = 4861$ Å, [OIII] $\lambda = 4959, 5007$ Å, and [NI] $\lambda = 5197, 5201$ Å) redshifted according to the line-of-sight velocity of NGC 7217. Chilingarian (2009) demonstrated that Hβ contains 20 per cent of the age-sensitive information at maximum when using the NBursts technique in a spectral range similar to ours, therefore excluding it from the fit neither biases age estimates (see also Appendix A2 in Chilingarian et al. 2007b and Appendix B in Chilingarian et al. 2008), nor degrades significantly the quality of the age determination.

We fitted Gaussians pre-convolved with the SCORPIO LSF into the [OIII] and Hβ emission lines in the residuals of the stellar population fitting and determined the ionised gas kinematics independently in the two lines as well as the emission line flux ratios.

The obtained radial distributions of SSP-equivalent

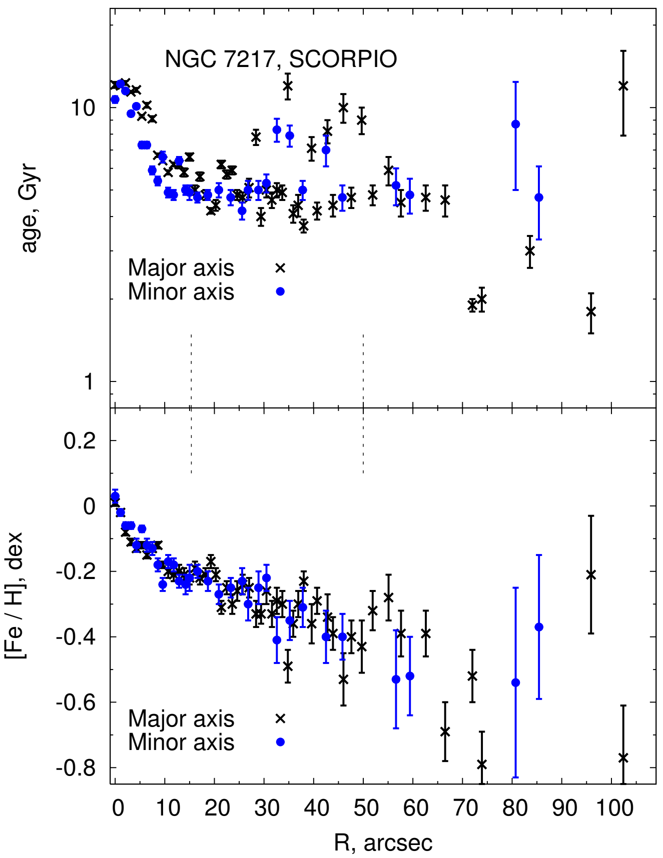

Figure 1. Radial distributions of the mean age (top) and metallicity (bottom) of the stellar populations measured along the major ($PA = 81^\circ$) and minor ($PA = 169^\circ$) axes. The vertical dashed lines indicate the conventional boundaries of the bulge and the inner exponential component set at four scalelenghts of each component.

age and metalliticity of NGC 7217 are shown in Fig. 1. Sil'chenko & Afanasiev (2000) analysed the large scale structure of NGC 7217 and identified three galaxy components, a bulge dominating at radii 5−15 arcsec (0.4–1.2 kpc), and two exponential structures interpreted as discs. The inner and outer discs dominate in the galaxy light profile at $20-50$ arcsec (1.6–4 kpc) and $60-110$ arcsec (4.8–8.8 kpc) respectively.

The age profile of NGC 7217 presented in Fig. 1 exhibits specific features at the radii dominated by these three substructures. In the bulge dominated region located mostly inside the nuclear starforming ring ($R = 10-12$ arcsec), the mean stellar age decreases from 10–13 Gyr in the centre to 5 Gyr outwards. In the inner exponential component the age stays nearly constant at about 5 Gyr; individual estimates at the radii between 20 and 50 arcsec have rms of 0.7 Gyr in the major-axis profile and 0.9 Gyr in the minor-axis one. The outer exponential component ($R = 60-110$ arcsec) has an intermediate age of about 2–3 Gyr, whereas in the broad outer starforming ring ($R = 70-80$ arcsec) it drops down to 1 Gyr. Surprisingly, at these radii we also see a drop in the SSP-equivalent stellar metallicity down to −0.65 dex prominent in the eastern side of the galaxy but hardly detected in the western side, which is probably connected to the morphology and location of individual starforming regions crossed by the slit. The mean metallicity of the bulge is close to the solar value, [Fe/H]=−0.06 dex, while the outer exponential component ([Fe/H]=−0.45 dex) is rather metal poor for such a massive galaxy. The inner exponential component has a mean metallicity of about −0.2 dex with a notable metallicity gradient around −0.3 dex per dex in radius.

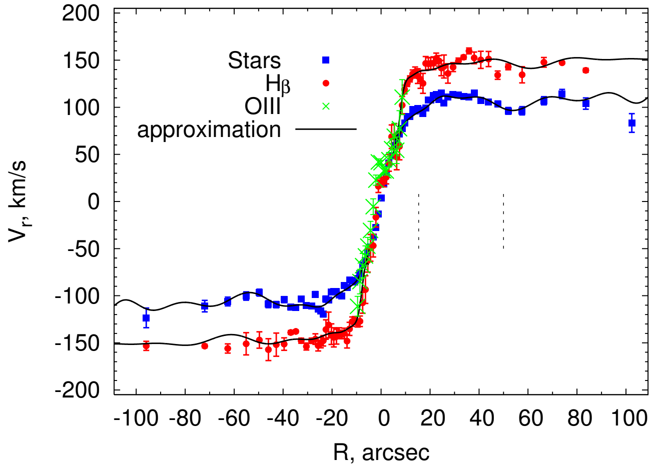

Figure 2. Radial distribution of the line-of-sight velocities of stars and ionized gas along the major ($PA = 81^\circ$) axis. The [OIII] data are presented only for $|R| < 10$ arcsec. The vertical dashed lines indicate the conventional boundaries of the bulge and the inner exponential component (see Fig. 1).

Hence, the existence of the three components found in the photometric data by Sil'chenko & Afanasiev (2000), a bulge and two [probably] exponential discs, is supported by specific features in the stellar population profiles. Later, we will propose the evolutionary scenario of NGC 7217, where the two discs may have different origin.

We present the derived major axis (P.A.=81 deg) profiles of line-of-sight velocities for the gaseous and stellar components in Fig. 2. The Hβ emission line component remains clearly visible along the whole extent of the galaxy where we can measure the stellar kinematics. The [OIII] is much weaker than Hβ at radii $R > 10$ arcsec. The velocities obtained from the two emission lines agree well, but those determined from Hβ in the outer region have 4–5 times smaller uncertainties. Therefore, we constructed the combined gaseous line-of-sight velocity profile displayed in Fig. 2 from [OIII] and Hβ kinematics at radii below and above 10 arcsec correspondingly. Both, stellar and gaseous velocity profiles have similar shapes including even some particular features such as a notable drop at $R \approx 50$ arcsec. They are also very symmetric. Therefore, for the dynamical analysis presented in the next section, we folded them along the galaxy centre and averaged the values of rotation velocities from both sides. The gaseous rotation velocities ($\sim$ 150 km s^{-1}) exceed the stellar ones ($\sim$ 120 km s^{-1}) by nearly 30 km s^{-1} at all radii, which is an observational manifestation of the asymmetric drift. The difference stays nearly constant between 10 and 70 arcsec suggesting similar dynamical statuses of the inner and outer exponential stellar structures. These structures are probably discs, but quite

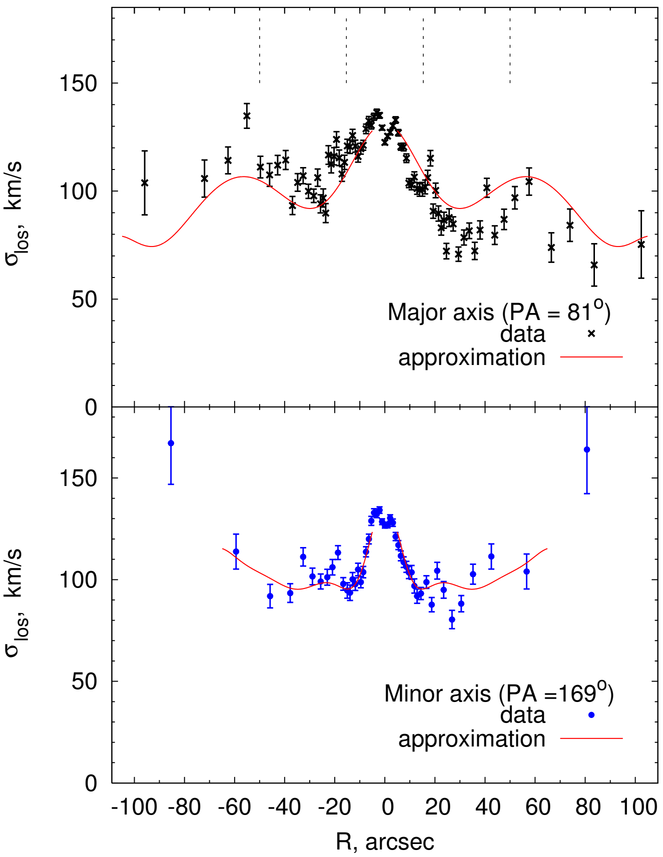

Figure 3. Radial distributions of the line-of-sight stellar velocity dispersion measured along the major, $PA = 81°$, (top) and minor, $PA = 169°$, (bottom) axes. The vertical dashed lines indicate the conventional boundaries of the bulge and the inner exponential component (see Fig. 1).

high asymmetric drift implies that they should be rather thick.

In Fig. 3 we show the observed radial distributions of the line-of-sight stellar velocity dispersion along minor and major axes of NGC 7217. Since the galaxy is seen nearly face-on, the vertical (σ_z) component of the disc velocity ellipsoid creates the main contribution to the observed velocity dispersion. However, there is a notable difference between major- and minor-axis velocity dispersion profiles suggesting significant contributions of the tangential (σ_φ) and radial (σ_R) velocity dispersions to the values along the major and minor axes respectively. The main feature of the stellar line-of-sight velocity dispersion profiles of NGC 7217 is a minimum in the area of the inner exponential component and a smooth raise outwards. This behaviour is quite unexpected: as we demonstrated, the outer stellar component is younger than the inner one, so it would be more natural if the stellar subsystem formed recently from the dynamically cold gas is itself dynamically cold. However, the velocity dispersion rise beyond $R \approx 50$ arcsec is statistically significant and seen in both minor- and major-axis velocity dispersion profiles. In Section 5 we will give the possible explanation of these features.

4 DYNAMICAL ANALYSIS: TWO VERY DIFFERENT DISCS IN NGC 7217

We used our kinematical data to recover the stellar velocity ellipsoid and reconstruct the radial distributions of all stellar velocity dispersion components. Then, we calculated the stellar disc thickness profile from the σ_z radial distribution. By using relations describing the disc equilibrium, we did it independently from the major- and minor-axis kinematical data.

For an intermediately inclined galaxy, the two in-plane components of the stellar velocity dispersion, σ_R and σ_φ, are related to the observed minor- and major-axis line-of-sight velocity dispersions according to the following relations:

$$\begin{aligned} \sigma^2_{\rm los,min}(R\cos i) &= \sigma^2_R \sin^2 i + \sigma^2_z\, cos^2 i\,, \\ \sigma^2_{\rm los,maj}(R) &= \sigma^2_\varphi \sin^2 i + \sigma^2_z\, cos^2 i\,. \end{aligned} \tag{2}$$

They also include the contribution from the vertical component of the velocity ellipsoid σ_z. Thus, by measuring the variations in the line-of-sight dispersions along the principal axes, we can obtain only a linear combination of $\sigma_R(R)$, $\sigma_\varphi(R)$ and $\sigma_z(R)$. Therefore, we need additional information in order to derive all three velocity dispersion components from these equations. To close the system of equations (2), we can use some dynamical relations, which are valid if the system is in equilibrium. One such relation connects the velocity dispersion components $\sigma_R(R)$ and $\sigma_\varphi(R)$ via the mean azimuthal velocity of stars (Binney & Tremaine 1987)

$$\frac{\sigma^2_\varphi}{\sigma^2_R} = \frac{1}{2}\left(1 + \frac{\partial \ln \bar{v}_\varphi}{\partial \ln R}\right)\,. \tag{3}$$

If the rotational velocities are unknown, we can use the local circular speed of gas $v_{\rm c}$ instead of $\bar{v}_\varphi$ in order to relate σ^2_R and σ^2_φ

$$\frac{\sigma^2_\varphi}{\sigma^2_R} = \frac{1}{2}\left(1 + \frac{\partial \ln v_{\rm c}}{\partial \ln R}\right)\,. \tag{4}$$

This relation is true if most orbits in a disc are quasi-circular.

Adding any of these relations, Eq. 3 or Eq. 4, to the two presented above, enables us to recover radial distributions of all three velocity dispersion components. For the first time this technique was applied to the data for NGC 488 by Gerssen et al. (1997). However, this procedure creates very noisy output when applied directly to the data, because it includes the subtraction of the two quantities $\sigma^2_{\rm los,min}$ and $\sigma^2_{\rm los,maj}$ with very close values, as well as the numerical derivation of $\bar{v}_\varphi$ or $v_{\rm c}$. A possible solution is to parametrize the kinematical profiles and to find the best fitting solution (see e.g. Gerssen et al. 1997, 2000; Shapiro et al. 2003) which will, however, depend on the adopted parametrization. For this reason, we adopted the less parametric approach as in Noordermeer et al. (2008). We approximated all kinematical profiles using polynomials and calculated all quantities including their derivatives analytically. But even then, the subtraction of the major axis velocity dispersion profile from the minor axis one results in unreliable and ambigious solution. To avoid this, we use the asymmetric drift equation. The deprojected major-axis gas rotation is a measure of the circular speed $v_{\rm c}$, while the deprojected major-axis stellar velocities allow us to determine the mean rotational motion $\bar{v}_\varphi$ related to the radial velocity dispersion

σ_R. Therefore, we can obtain the σ_R profile using the major-axis velocity profiles for gas and stars and the asymmetric drift equation (Binney & Tremaine 1987):

$$v_{\rm c}^2 - \bar{v}_\varphi^2 = \sigma_R^2 \left(\frac{\sigma_\varphi^2}{\sigma_R^2} - 1 - \frac{\partial \ln \Sigma}{\partial \ln R} - \frac{\partial \ln \sigma_R^2}{\partial \ln R} \right) , \qquad (5)$$

where Σ is the stellar surface density. Provided that the stellar mass-to-light ratio stays nearly constant ($(M/L)_I = 1.86$ in the Solar units from the PEGASE.2 models, see Fioc & Rocca-Volmerange 1997), we can use the surface brightness instead of surface density Σ in Eq. 5. We assume that the I-band photometric data trace old stellar population whose internal kinematics we are studying. Because of the logarithmic derivative, the exact choice of the M/L ratio is not critical. The asymmetric drift equation can be used directly to obtain the radial velocity dispersion profile, provided that the ratio between $\sigma_\varphi^2/\sigma_R^2$ is determined from Eq. 3 or Eq. 4. However, Eq. 5 requires the knowledge of the σ_R radial gradient. We assume that in the outer regions of the galaxy between 30 and 70 arcsec, σ_R may decline exponentially as $\propto \exp(-R/h_{\rm kin})$ and use the last term in the form $2R/h_{\rm kin}$, where $h_{\rm kin}$ is a free parameter.

The choice of a radial velocity dispersion profile exponentially declining with the radius is physically motivated. There is a conventional assumption that the disc thickness and the z-component of the velocity dispersion σ_z are connected via the vertical equilibrium condition for an isothermal layer (Spitzer 1942)

$$\sigma_z^2(R) = \pi\, G\, \Sigma(R)\, z_0 \,, \qquad (6)$$

where z_0 is the half-thickness of a homogeneous layer. For a mass-to-light ratio constant with radius, constant z_0 and an exponential brightness profile it yields:

$$\sigma_z^2(R) \propto \exp(-R/h) \,, \qquad (7)$$

where h is a disc scalelength.

The disc heating theory suggests that the range in the velocity anisotropy σ_z/σ_R is about $0.4 - 0.8$ (Jenkins & Binney 1990), which is consistent with observations. Gerssen et al. (1997, 2000) and Shapiro et al. (2003) modelled the data for several galaxies and estimated the values for the velocity anisotropy σ_z/σ_R between 0.5 and 0.7, similar to the solar neighbourhood (Dehnen & Binney 1998).

Since the ratio σ_z/σ_R is close to constant, Eq. 7 yields:

$$\sigma_R \propto \exp(-R/2\,h) \,. \qquad (8)$$

It implies that $h_{\rm kin} = 2\,h$. This approach does work for our Galaxy (Lewis & Freeman 1989) but in the case of NGC 7217 we did not fix the value of $h_{\rm kin}$ and estimated it iteratively by fitting the radial velocity dispersion profile with the exponential law and substituting the value of $h_{\rm kin}$ in the asymmetric drift equation. We needed this value to estimate only the last term in Eq. 5. The exact value of this term may affect the final results but the effect it quite insignificant. We were changing the range of R used to fit σ_R by exponential law and did not notice any difference between final results. Having derived the σ_R radial distribution from the Eq. 5, we can then compute the radial profile of the vertical component of the velocity dispersion σ_z using one of the Eq. 2. We choose to use both of them to control the reliability of our results.

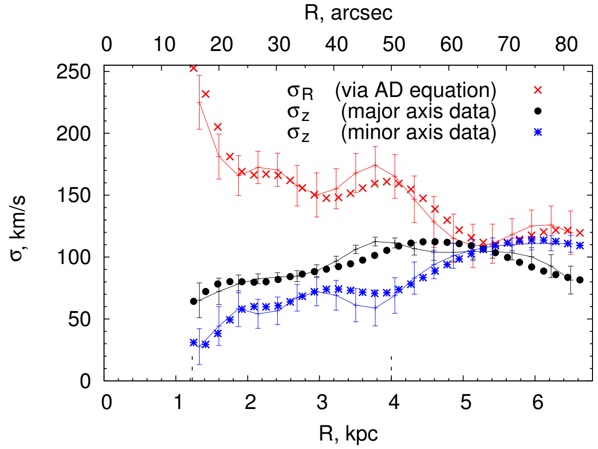

Figure 4. Radial distributions of the radial and vertical velocity dispersions reconstructed from the major- and minor-axis kinematical profiles. Full lines – profiles calculated via the Eq. 3, symbols – profiles obtained by using the Eq. 4. Error bars are shown only for profiles indicated by solid lines. The vertical dashed lines indicate the conventional boundaries of the bulge and the inner exponential component (see Fig. 1).

Finally, we can obtain the thickness profile from Eq. 6 which is valid for an isothermal layer. The assumption about constant velocity dispersion along the z-direction for discs is in agreement with the results of N-body simulations (see e.g. Fig. 2 in Sotnikova & Rodionov 2006). But one should keep in mind that Eq. 6 gives the upper limit for the disc thickness. If there is a massive dark halo, the disc thickness will be lower for the same value of σ_z.

In order to deproject the velocity profiles we need to know the inclination of the rotation plane to the line of sight. NGC 7217 has a roundish appearance, however quite high observed (i.e. projected) rotation velocities suggest that is not seen completely face-on. The isophote ellipticity analysis assuming the infinitely thin stellar disc provided the disc inclination estimates in the range of $i = 26 - 28$ deg (Noordermeer & van der Hulst 2007; Verdes-Montenegro et al. 1995; Sánchez-Portal et al. 2000); whereas the kinematical analysis usually results in slightly higher values $i = 30 - 31$ deg (see Buta et al. 1995; Noordermeer et al. 2005 for the HI map analysis and Sil'chenko & Moiseev 2006 for the stellar kinematics). Keeping in mind possible considerable thickness of the stellar disc, we adopt the inclination value of $i = 30$ deg. Varying i between 26 and 35 deg changes the resulting disc thickness estimates by no more than 10 per cent.

We present the reconstructed radial distributions of σ_R and σ_z in Fig. 4. We estimated uncertainties using a bootstrapping method (Press et al. 1992). We computed σ_R and σ_z assuming that the errors of observational quantities used in the procedure are distributed according to the normal law and changing input data points according to these errors. We made several thousands realisation of the procedure, averaged resulting values, and estimated the dispersion of all the simulations at each point.

The data in the Fig. 4 suggest that the dynamically coolest subsystem of NGC 7217 as concerning the vertical velocity dispersion is the *inner* stellar exponential component. Therefore it is certainly a disc and not a pseudo-

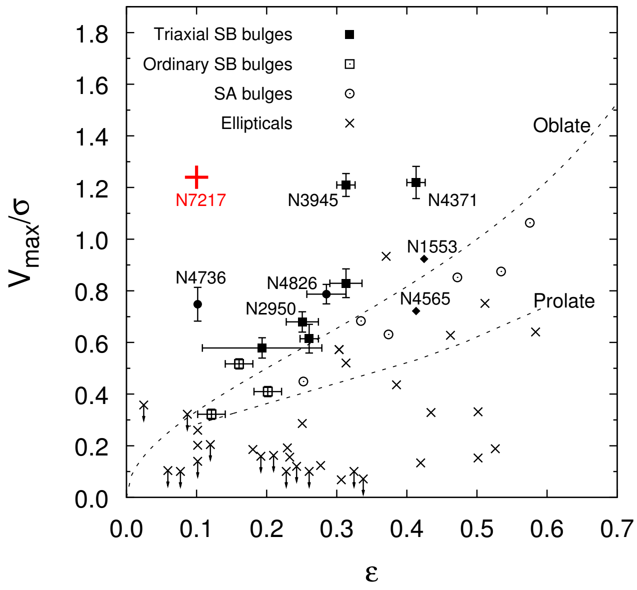

Figure 5. Relation between the ratios of observed maximal rotation velocities and velocity dispersions and isophote ellipticities for early-type galaxies, bulges (open symbols) and pseudobulges (filled symbols). The models of prolate and oblate isotropic rotators are overplotted by dashed lines. NGC 7217 is shown with a red cross being clearly above the locus of pseudobulges from Kormendy & Kennicutt (2004).

bulge. Indeed, in Fig. 5 we plot the inner exponential component of NGC 7217 at the diagram of Binney–Kormendy. With its $\epsilon \approx 0.1$ and $v_{\rm max}/\sigma_{\rm los} = 1.24$ it stays well above all the pseudobulges dynamically confirmed by Kormendy. At $R > 30$ arcsec (>2.4 kpc) the vertical velocity dispersion component slowly raises along outwards reaching 110 km s^{-1} at the location of the outer starforming ring. The σ_R profile decreases along the radius as expected, but in the transition region where the outer disc starts to dominate ($R = 40 - 50$ arcsec; 3.2–4.0 kpc), we see a break of the monotonic fall. The whole σ_R profile can be divided into two parts corresponding to the two exponential stellar components.

The disc "thickness profiles" at radii $R = 15 \ldots 80$ arcsec reconstructed from the major- and minor-axis kinematics are shown in Fig. 6. While the qualitative agreement between them exists, quantitatively they diverge at some radii. As it was mentioned in Section 2, the minor axis data are of a worse quality than the major axis ones but they are featureless as concerning the line-of-sight stellar velocity dispersion. In this sense, both datasets are worth each other. One of the sources of the profile discrepancy might be the adopted inclination angle and the discrepancy between measured distances along the major axis and deprojected distances along the minor axis. Similarly to the σ_z profile behaviour, we see that the inner stellar disc is relatively thin ($z_0 = 0.2 \ldots 0.7$ kpc). Hence, at its inner boundary the ratio of its scalelength to the scaleheight is about 4–5. The outer disc flares vigorously reaching the half-thickness of 2.5-3 kpc at the outer starforming ring position.

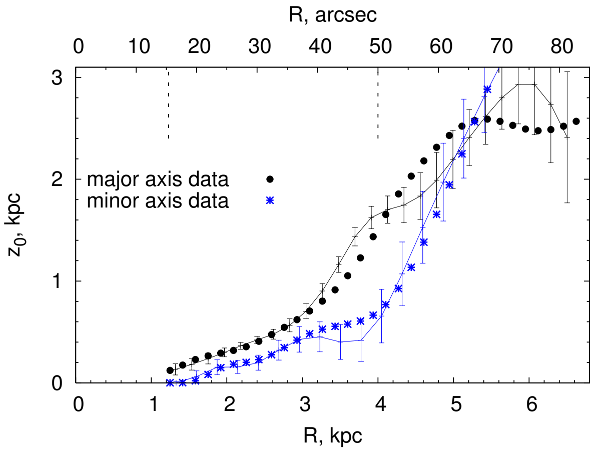

Figure 6. Radial distribution of the stellar disc scaleheight – the reconstructed "edge-on" view. Solid lines are the profiles calculated via Eq. 3, while symbols are for the profiles obtained by using Eq. 4. Error bars are shown only for profiles indicated by solid lines. The vertical dashed lines indicate the conventional boundaries of the bulge and the inner exponential component (see Fig. 1).

5 DISCUSSION

5.1 Explaining the structure of NGC 7217

From the analysis of the stellar and gaseous kinematics (line-of-sight velocities and velocity dispersion radial distributions) over an extended area of the giant early-type disc galaxy NGC 7217, we reconstructed the velocity ellipsoid and calculated the stellar disc scaleheights at radii from 20 to 70 arcsec (1.6 to 6 kpc). Earlier, Sil'chenko & Afanasiev (2000) demonstrated that this radial range contains two stellar substructures having exponential surface brightness profiles with different scalelengths, the inner one with relatively low h, and the outer one with more extended (standard for giant galaxies) scalelength. Our analysis reveals that the inner component has the scaleheight of 0.2–0.7 kpc and the outer one about 1–3 kpc. Hence, we can classify the inner and outer components as thin and thick stellar discs respectively.

Having applied the full spectral fitting NBursts technique with a grid of high-resolution SSP models, we deduced mean ages and metallicities of stars. The inner disc exhibits the intermediate age of about 5 Gyr and the mean metallicity of -0.2 dex with a strong negative metallicity gradient along the radius. The outer disc is quite metal-poor ([Fe/H]$= -0.4$ dex) and relatively young (2 Gyr). The outer disc harbours a prominent starforming ring with the mean age of about 1 Gyr at the radius of $R \approx 75''$ very well visible in UV data from the GALEX satellite and 8μm NIR data from the Spitzer Space Telescope. Interestingly, in this ring the mean stellar metallicity falls down to a very low value of -0.7 dex. The galaxy nucleus and the bulge of NGC 7217 inside the nuclear starforming ring are very old ($\sim 13 - 15$ Gyr).

How can we explain the complex structure of NGC 7217? In principle, the fact that the outer stellar disc is younger than the inner one is in line with the paradigm of the 'inside-out' disc formation. But the sharp boundary between the two discs, where the properties including stellar

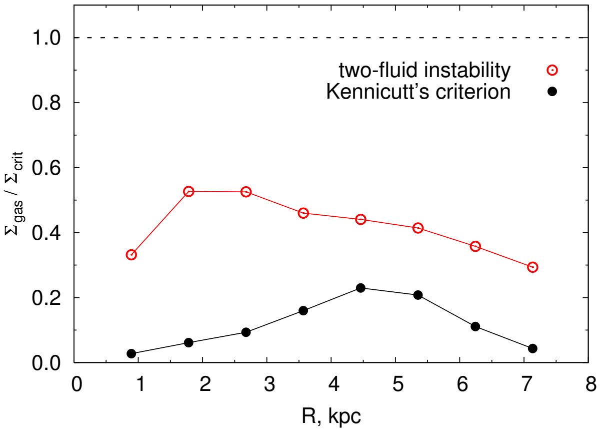

Figure 7. Ratio between observed gas density and critical density according to Kennicutt (1989) and the two-fluid instability (Jog & Solomon 1984; Efstathiou 2000) criteria. The dashed line indicates the threshold for star formation. The HI surface density profile was taken from Noordermeer et al. (2005).

age and metallicity as well as the radial and vertical scalelengths of the star distribution change abruptly, hints to a temporal gap between the inner and outer disc formation, or to some catastrophic event that provoked the expansion of star formation into the outer ring area.

Interestingly, the molecular gas concentrates in the inner disc (Combes et al. 2004) while the neutral hydrogen is observed in the narrow ring in the outer disc (Verdes-Montenegro et al. 1995; Buta et al. 1995; Noordermeer et al. 2005). However, star formation is almost absent in the inner disc (though it burns in the nuclear starforming ring between the bulge and the inner disc) and is very prominent in the outer disc (Battinelli et al. 2000). Noordermeer et al. (2005) estimated the gravitational stability of the gas in the outer ring and the threshold density for star formation according to the Kennicutt (1989) criterion,

$$\Sigma_{\rm cr} = \alpha \, \frac{\kappa c}{3.36 G} \, , \qquad (9)$$

where κ is the epicyclic frequency, that can be derived from the rotation and c is the gas velocity dispersion, which can be assumed as a constant value of 6 km s^{-1}. For the dimensionless quantity α, Kennicutt derived a value of 0.67 from the empirical study of star formation cutoffs in spiral galaxies. Dynamically, it means that one should take into account non-axisymmetric modes while considering the stability of a disc, because for axisymmetric modes $\alpha = 1$ (Toomre 1964). Noordermeer et al. (2005) demonstrated that even in the middle of the HI ring of NGC 7217, the gas density does not exceed 25 per cent of the critical one. The estimate by Noordermeer et al. (2005) did not take into account the existence of a stellar disc. Having restored the velocity dispersion profile σ_R for stars, we can evaluate the gaseous disc stability in the framework of the two-fluid approach (Jog & Solomon 1984; Efstathiou 2000)

$$\Sigma_{\rm cr} = \frac{\kappa c}{3.36 G g(a,b)} \, , \qquad (10)$$

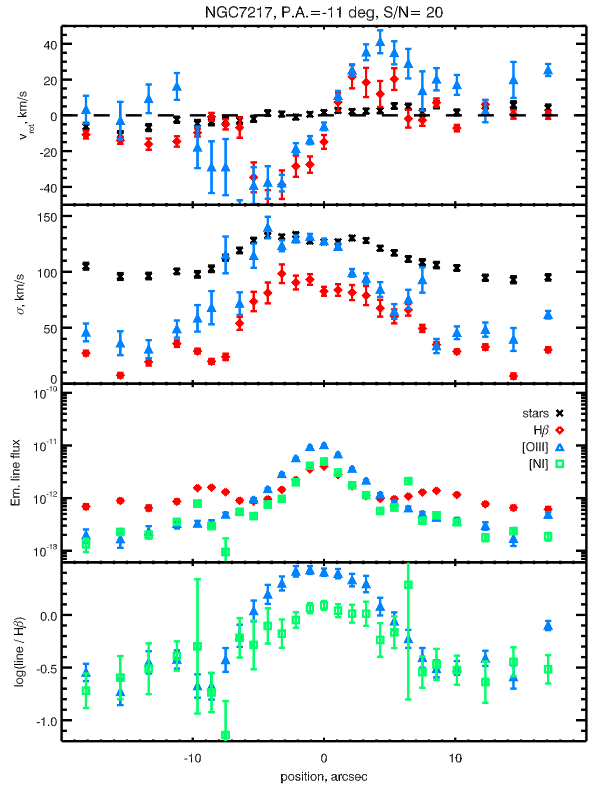

Figure 8. Minor-axis kinematics and emission line properties of NGC 7217 from the analysis of the Hβ (red, diamonds), [OIII] ($\lambda = 5007$ Å, blue, triangles), and [NI] ($\lambda = 5197/5200$ Å, green, squares) lines in its spectra with the best-fitting stellar population models subtracted. The panels show (top to bottom): radial velocities, velocity dispersion, line fluxes, logarithms of the emission line ratios: [OIII]/Hβ (blue) and [NI]/Hβ (green).

where a and b are the ratios of stellar to gas velocity dispersion and surface densities respectively, and $g(a,b)$ is a function derived numerically by Efstathiou (2000). This approach results in the critical density estimate at least twice lower than the value obtained by Noordermeer et al. (2005). But even now the critical density remains too high (see Fig. 7). Therefore, the gas in the outer ring must be gravitationally stable, and why the star formation proceeds there is still an open question. The very existence of a system of starforming, gas-populated rings in an unbarred galaxy is a puzzle. Combes et al. (2004) discussed a possibility of a past bar, strong or weak, which had formed the rings and then had dissolved after the gas inflow had supplied mass into the center. Now we see that this scenario experiences strong difficulties: the stellar population in the NGC 7217 centre is very old, and it is clear that no significant star formation took place there for the last 5 Gyr in order to provide mass concentration and the subsequent bar destruction.

5.2 Inner polar disc

In Fig. 8 we present the minor-axis kinematics and emission line properties in the central region of NGC 7217 derived from the analysis of the stellar population spectral fitting residuals. In the nuclear region the [NI] doublet is clearly detected in addition to the oxygen and hydrogen lines. The [OIII] kinematics is evident of either a rotating disc or an outflow from the galaxy centre which can be in-

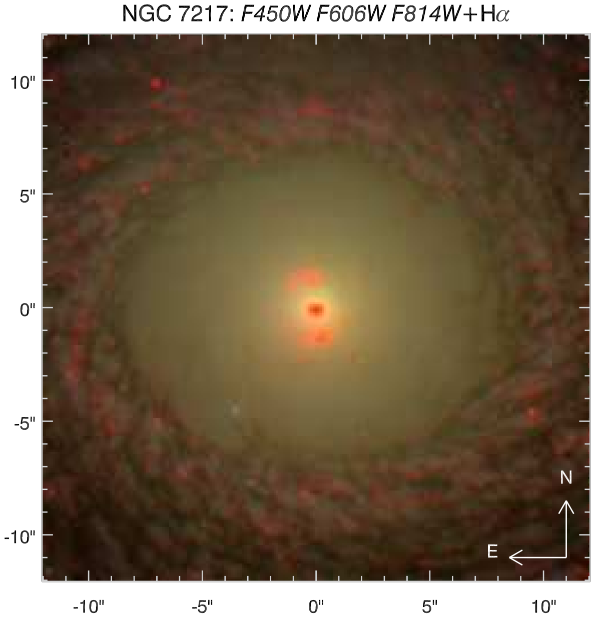

Figure 9. Inner polar disc in NGC 7217 as seen with the HST. This false colour composite is made of $F450W$, $F606W$, and $F814W$ WFPC2 images with the Hα fluxes from the ACS $F658N$ images added to the red channel using the Lupton et al. (2004) algorithm. The strongly inclined gaseous structure seen here in the centre is a polar disc because the outer disc is seen almost face-on with its major axis nearly horizonthal in this plot.

duced by an active nucleus. We measured the emission line ratios (see bottom panel in Fig. 8) and used the ITERA tool (Groves & Allen 2010) providing a large collection of emission line models for different excitation mechanisms to perform the diagnostics. The extremely high $\log([\mathrm{N\,I}]/\mathrm{H}\beta) > 0$ ratio given moderate $\log([\mathrm{O\,III}]/\mathrm{H}\beta) \approx 0.45$ is consistent with either a shock ionisation for solar or subsolar metallicities of the ISM, or an AGN having a significantly supersolar metallicity (e.g. $> +0.3$ dex). Given very moderate metallicity of the stellar population in the central region of NGC 7217, the latter possibility can be ruled out at a high level of confidence. Therefore, we are probably observing an inner polar disc in NGC 7217, which is supported by the direct inspection of the HST imaging data in the narrow Hα+[NII]λ6583-centered filter (Fig. 9).

According to Karachentseva (1973), NGC 7217 is an isolated galaxy, not a member of any group, and its environment is empty of satellites. However, Merrifield & Kuijken (1994) and Sil'chenko & Afanasiev (2000) suggested the presence of a counterrotating stellar component in the central region of NGC 7217; moreover, we see also the inner polar gaseous disc. Hence, accretion or minor merger(s) in the past seem inevitable. If we assume that the galaxy centre is its oldest part then we can suspect the vertical impact by a gas-rich satellite. Then the 0.3 kpc nuclear polar disc in NGC 7217 is a remnant of the satellite gaseous component which conserved its initial orbital momentum. The close analogue of such an event is the Sagittarius dSph disruption by the Galaxy accompanied by the re-distribution of the satellite material along the polar large circle. Polar orbits are known to be stable, hence this gas cannot accrete to the very centre explaining why the fuel for the star formation in the centre of NGC 7217 has been absent until now evidenced by the old stellar population there.

Such a vertical impact is also able to produce a system of starforming/stellar rings by exciting a running compression wave in a large scale galaxy disc (Athanassoula et al. 1997). Moreover, the simulations of a Cartwheel-like galaxy by Mapelli et al. (2008) for 1.5 Gyr after the impact clearly show that sharp stellar rings formed initially expand over a large area during 1 Gyr and form a structure resembling a low surface brightness outer stellar disc. The two-tiered exponential stellar disc of NGC 7217 could have been built by such a minor merger. But we still need a triaxiality of the potential in order to produce a counterrotating component in the inner disc during the same event: the polar gas in the tumbling triaxial potential has to warp in the outer part in such a sense that it arrives to the rotational plane of stars with the opposite spin (van Albada et al. 1982). Being compressed, this gas would be consumed by star formation leaving a counterrotating stellar component. Besides, the triaxial potential also creates long-living resonance rings in contrast to short-living collisional rings. From our data we cannot distinguish between a triaxial dark-matter halo and a low-contrast extended stellar spheroid (see discussion in Buta et al. 1995).

5.3 Insights from simulations

Simulations of vertical impacts producing ring structures reveal that the vertical oscillations of disc stars excited by the intruder's passage result in strong thickening of the stellar disc (Hernquist & Weil 1993) which we probably observe in the outer disc of NGC 7217. The small thickness of the inner disc can be perhaps explained by its high density increased after the impact by the counterrotating component and also by the presence of the significant molecular gas content (Combes et al. 2004). Interestingly, in the recognized vertical collision product, the famous Cartwheel galaxy, the molecular gas concentrates in the central region while the neutral atomic hydrogen is confined to the outer ring (Horellou et al. 1998) being very similar to NGC 7217.

One can suggest another explanation of the inner disc structure. It could have been formed from the material of a small satellite during its complete disruption (Eliche-Moral et al. 2006). This new inner disc can be older than the outer one because the infalling stars were initially older. It can also be dynamically cold because its material had experienced the orbital circularisation. However, this scenario requires a nearly in-plane encounter. The unusually high thickness of the outer component and the presence of the inner polar disc in NGC 7217 make us to prefer encounters at higher inclinations.

The minor merger scenario with a vertical impact requires this event to have occurred long time ago. The galaxy needs time to convert the counterrotating gas into stars and to establish the mean stellar age of 5 Gyr in the compact high-density inner stellar disc. Then the current star formation in the outer disc involving very low-metallicity gas does not relate to this event and to its collision rings. It may be provoked by later gas infall in a tidal tail developped during the minor merger. This mechanism can explain the patchy and filamentary edges of the HI ring in the map of

NGC 7217 (Noordermeer et al. 2005) and the presence of the shock-induced star formation in the low-density gas ring which had to be gravitationally stable under the quiescent conditions.

We explored intermediate resolution (0.2 kpc) TreeSPH simulations of minor mergers provided by the GalMer database[3] (Chilingarian et al. 2010). Presently available simulations include interactions of a gas free giant lenticular galaxy ("gS0") with a 10 times less massive dwarf galaxy. The morphology of a dwarf spans the entire Hubble sequence from non-rotating ellipticals ("dE0") to bulgeless discs ("dSd"). Here we consider only gS0–dSd mergers, as this configuration has the largest quantity of gas compared to other morphologies of a satellite galaxy. The inclination of the orbital plane to the rotation planes of the two interacting galaxies is 33 deg for a giant S0 and 130 deg for dSd. The two sets of numerical experiments include interactions on prograde and retrograde orbits with different initial orbital momenta and motion energies (24 in total). The simulations were run for a total duration of 3 Gyr.

The bar is always formed in the gS0 stellar disc. Merger remnant morphologies vary quite a lot, but all of them can be classified into two families related to the mutual orientation of the infalling satellite internal angular momentum with respect to that of the orbital motion.

All retrograde encounters result in the formation of a strongly inclined inner starforming ring in the gS0 galaxy having a radius of ≈ 1 kpc. Its plane is orthogonal to the initial orbital plane of an interaction, i.e. its inclination to the gS0 disc plane is about 60 deg. This ring is located in the inner bright part of the S0 bulge and its contribution to the total stellar light (and, consequently, to the stellar kinematics derived from the spectra) in the central region of the galaxy is negligible (see left panel of Fig. 10). However, it is immediately revealed by the gas kinematics (see right panel of Fig. 10), as it is the only structure with significant gas content. Although the mass ratio of 1:10 in *total mass* is quite high, none of the retrograde encounters heated up significantly the large scale S0 disc.

The situation is totally different for prograde encounters. They heat and thicken the gS0 disc significantly, nearly destroying it for certain orbital types with high motion energies. The gas and newly formed stars from the infalling satellite form a large scale co-rotating disc in the main plane of the gS0 galaxy or between its initial plane orientation and the orbital plane if the large scale stellar disc is destroyed. If the large disc survives, the gas is concentrated at one of its resonances, probably the outer bar resonance, creating a starforming ring having $R \approx 8$ kpc quite thick (~ 1 kpc) in the radial direction (see Fig. 11). As it resides in a region where the surface density of the gS0 disc is rather low, it creates significant contribution to the galaxy light. Since the initial metallicity of the interstellar medium in dSd is low, the newly formed stars in this ring will also have low metallicities being in agreement with young metal poor stars detected by our stellar population analysis in the outer ring of NGC 7217. Worth mentioning that due to the intense heating, the large scale gS0 disc flares in the outer regions of a galaxy (see Fig 12). The outer disc must have formed by this event not very long time ago, otherwise we would have expected to see young metal-poor stars formed in it migrating inwards and erasing an observed quite sharp break in the age profile. The characteristic migration time of about 1 Gyr in a Milky Way-like galaxy using the mechanism proposed recently by Minchev & Famaey (2010) and Minchev et al. (2011) allows us to constraint the formation epoch of the outer disc of NGC 7217.

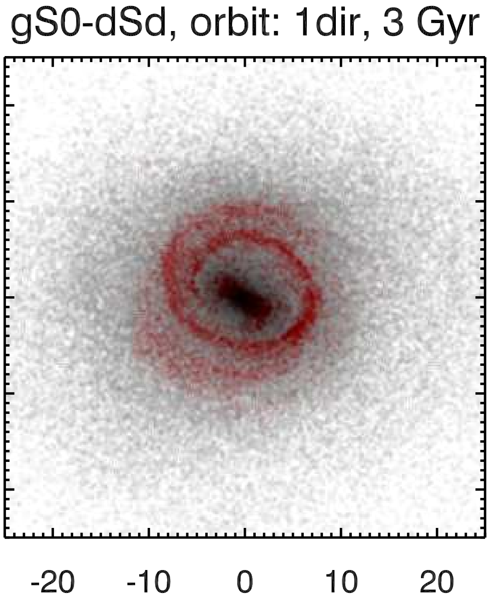

Figure 11. Surface density of stars (grayscale) and gas (red) for a minor wet merger of gS0 and dSd galaxies (mass ratio 10:1) on a prograde (direct) orbit. The orientation of the galaxy disc is chosen to match that of NGC 7217 ($i = 30$ deg). The axes are in kpc.

Hence, we conclude that the scenario of two consequent minor mergers at different orbits provides a plausible explanation to the observed structure of NGC 7217.

6 SUMMARY

We performed the analysis of internal kinematics and stellar population properties in the nearby isolated early-type disc galaxy NGC 7217 having star-forming rings by the NBURSTS full spectral fitting of deep long-slit intermediate resolution spectroscopic data.

The age and metallicity profiles of NGC 7217 exhibit three components that well correspond to those found in the structural analysis of the galaxy by Sil'chenko & Afanasiev (2000): an old metal-rich bulge dominating at radii 0.4–1.2 kpc, the inner disc with the mean age of 5 Gyr and slightly subsolar metallicity at 1.6–4 kpc, and the outer metal-poor relatively young disc (t =2–3 Gyr) beyond 4.8 kpc.

We analysed the parametrized major- and minor-axis kinematical profiles of NGC 7217, recovered the velocity ellipsoid in the regions dominated by the exponential discs and obtained the scaleheight radial profile. We concluded that the inner disc is thin ($z_0 = 0.2 \ldots 0.7$ kpc) while the

---

[3] http://galmer.obspm.fr/

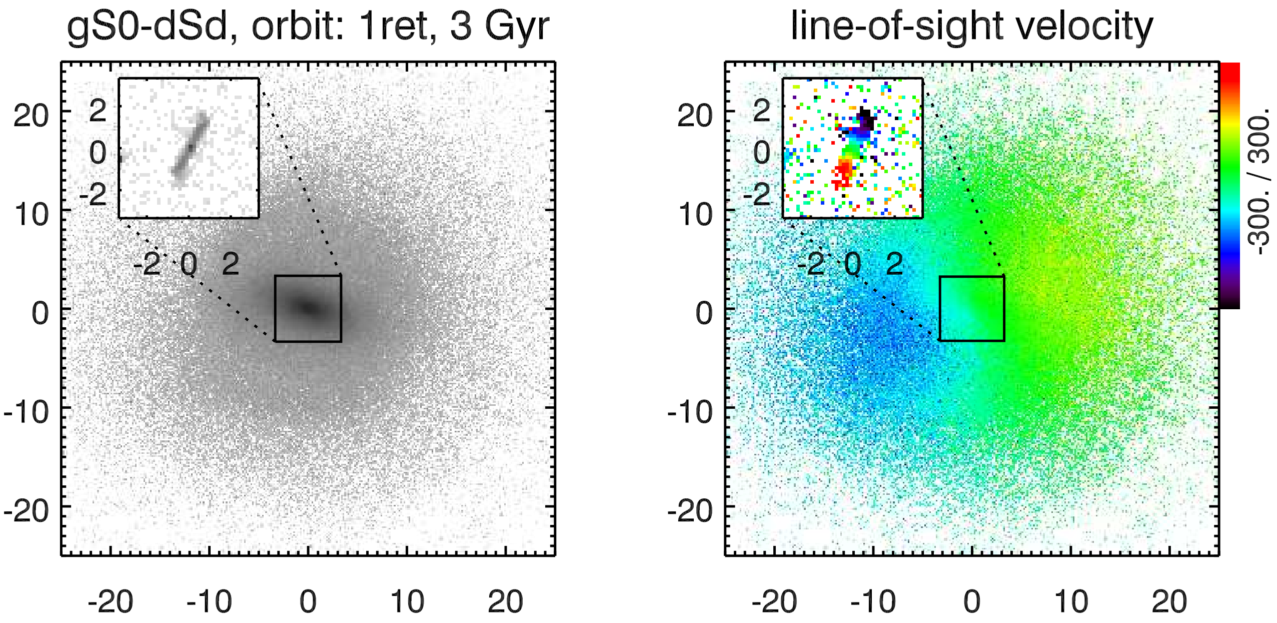

Figure 10. *Left panel:* surface density of stars and gas (inset) for a minor wet merger of gS0 and dSd galaxies (mass ratio 10:1) on a retrograde orbit. *Right panel:* line-of-sight velocities of stars and gas (inset) for the same merger. The signature of the inner polar ring seen edge-on is clearly visible. The orientation of the galaxy disc is chosen to match that of NGC 7217 ($i = 30$ deg). The axes are in kpc.

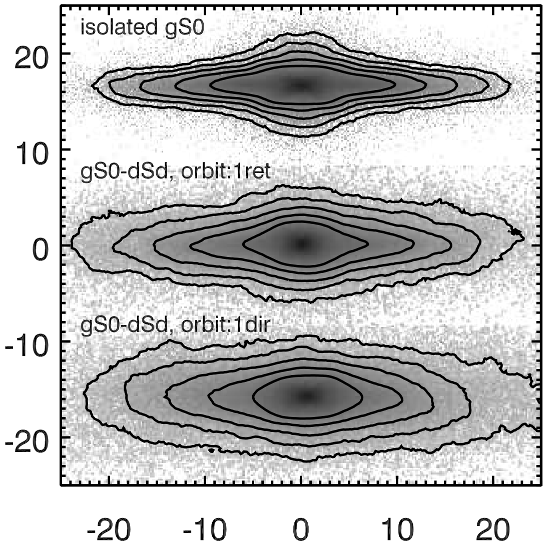

Figure 12. Disc thickening by minor mergers. The edge-on view of the GalMer model of a giant S0 galaxy in isolation is shown on top, the remnants of minor mergers with a gas-rich dSd galaxy (mass ratio 10:1, orbit type 1, see text) on retrograde and prograde orbits are displayed in the middle and in the bottom respectively. The contours are every 1 mag arcsec^{-2}, the axes are in kpc.

outer disc flares reaching the half-thickness of 2.5 kpc in the region of the outer starforming ring. Using the two-fluid approach, we evaluated the gaseous disc stability in NGC 7217 and showed that even the highest-density neutral-hydrogen ring at $R = 6$ kpc should be stable.

From the analysis of emission line ratios in the residuals of the spectral fitting of NGC 7217, we ruled out a strong nuclear activity as the mechanism of circumnuclear gas excitation and concluded that the peculiar ionized-gas kinematics in the central region of NGC 7217 was due to the presence of the inner polar disc.

By comparing our data with the numerical simulations of wet minor mergers in the GalMer database, we explained the observed structure and kinematics of NGC 7217 by the two consequent minor mergers with satellites having different initial orbits. The encounter on a retrograde orbit resulted in the formation of the inner polar disc, while the outer star-forming ring and the outer disc thickening were consistent with a minor merger on a prograde orbit.

ACKNOWLEDGMENTS

We thank Alexei Moiseev for the useful discussions. We are indebted to Alister Graham for his consultation. We are also grateful to our anonymous referee whose suggestions helped us to improve the clarity and presentation of the results. This research is partly based on observations made with the NASA/ESA Hubble Space Telescope, obtained from the data archive at the Space Telescope Science Institute, which is operated by the Association of Universities for Research in Astronomy, Inc., under NASA contract NAS 5-26555. The work on the study of young stellar rings in disc galaxies is supported by the grants of the Russian Foundation for Basic Researches number 10-02-00062a and number 09-02-00968a.

REFERENCES

Afanasiev, V. L. & Moiseev, A. V. 2005, Astronomy Letters, 31, 194

Andredakis, Y. C. & Sanders, R. H. 1994, MNRAS, 267, 283

Andredakis, Y. C., Peletier, R. F., & Balcells, M. 1995, MNRAS, 275, 874

Athanassoula, E., Puerari, I., & Bosma, A. 1997, MNRAS, 286, 284

Balcells, M., Graham, A. W., Domínguez-Palmero, L., & Peletier, R. F. 2003, ApJ, 582, L79

, Balcells, M., Graham, A. W., & Peletier, R. F. 2007, ApJ, 665, 1084

Battinelli, P., Capuzzo-Dolcetta, R., Hodge, P. W., Vicari, A., & Wyder, T. K. 2000, A&A, 357, 437

Bettoni, D., Galletta, G., & Prada, F. 2001, A&A, 374, 83

Binney, J. & Tremaine, S. 1987, Galactic Dynamics, (Princeton, NY, Princeton University Press)

Buta, R. & Crocker, D. A. 1993, AJ, 105, 1344

Buta, R., van Driel, W., Braine, J., Combes, F., Wakamatsu, K., Sofue, Y., & Tomita, A. 1995, ApJ, 450, 593

Cappellari, M. & Emsellem, E. 2004, PASP, 116, 138

Chilingarian, I. V. 2009, MNRAS, 394, 1229

Chilingarian, I., Prugniel, P., Sil'chenko, O., & Koleva, M. 2007a, in IAU Symposium, Vol. 241, Stellar Populations as Building Blocks of Galaxies, ed. A. Vazdekis & R. R. Peletier (Cambridge, UK: Cambridge University Press), 175–176, arXiv:0709.3047

Chilingarian, I. V., Prugniel, P., Sil'chenko, O. K., & Afanasiev, V. L. 2007b, MNRAS, 376, 1033

Chilingarian, I. V., Cayatte, V., Durret, F., Adami, C., Balkowski, C., Chemin, L., Laganá, T. F., & Prugniel, P. 2008, A&A, 486, 85

Chilingarian, I. V., Novikova, A. P., Cayatte, V., Combes, F., Di Matteo, P., & Zasov, A. V. 2009, A&A, 504, 389

Chilingarian, I. V., Di Matteo, P., Combes, F., Melchior, A., & Semelin, B. 2010, A&A, 518, A61+

Combes, F. & Sanders, R. H. 1981, å, 96, 164

Combes, F., et al. 2004, A&A, 414, 857

Dehnen, W. & Binney, J. J. 1998, MNRAS, 298, 387

Drory, N. & Fisher, D. B. 2007, ApJ, 664, 640

Efstathiou, G. 2000, MNRAS, 317, 697

Eliche-Moral, M. C., Balcells, M., Aguerri, J. A. L., & González-García, A. C. 2006, A&A, 457, 91

Erwin, P. & Sparke, L. S. 2002, AJ, 124, 65

Erwin, P., Beltrán, J. C. V., Graham, A. W., & Beckman, J. E. 2003, ApJ, 597, 929

Fioc, M. & Rocca-Volmerange, B. 1997, A&A, 326, 950

Freeman, K. C. 1970, ApJ, 160, 811

Friedli, D. & Benz, W. 1995, A&A, 301, 649

Gerssen, J., Kuijken, K., & Merrifield, M. R. 1997, MNRAS, 288, 618

Gerssen, J., Kuijken, K., & Merrifield, M. R. 2000, MNRAS, 317, 545

Graham, A. W. 2001, AJ, 121, 820

Groves, B. A. & Allen, M. G. 2010, New Astronomy, 15, 614

Hernquist, L. & Weil, M. L. 1993, MNRAS, 261, 804

Horellou, C., Charmandaris, V., Combes, F., Appleton, P. N., Casoli, F., & Mirabel, I. F. 1998, A&A, 340, L51

Ibata, R., Mouhcine, M., & Rejkuba, M. 2009, MNRAS, 395, 126

Jenkins, A. & Binney, J. 1990, MNRAS, 245, 305

Jog, C. J. & Solomon, P. M. 1984, ApJ, 276, 114

Karachentseva, V. E. 1973, Soobshcheniya Spetsial'noj Astrofizicheskoj Observatorii, 8, 3

Kennicutt, Jr., R. C. 1989, ApJ, 344, 685

Kormendy, J. 1993, in IAU Symposium, Vol. 153, Galactic Bulges, ed. H. Dejonghe & H. J. Habing, 209–+

Kormendy, J. & Kennicutt, Jr., R. C. 2004, ARA&A, 42, 603

Laurikainen, E., Salo, H., & Buta, R. 2005, MNRAS, 362, 1319

Le Borgne, D., Rocca-Volmerange, B., Prugniel, P., Lançon, A., Fioc, M., & Soubiran, C. 2004, A&A, 425, 881

Lewis, J. R. & Freeman, K. C. 1989, AJ, 97, 139

Lupton, R., Blanton, M. R., Fekete, G., Hogg, D. W., O'Mullane, W., Szalay, A., & Wherry, N. 2004, PASP, 116, 133

Mapelli, M., Moore, B., Ripamonti, E., Mayer, L., Colpi, M., & Giordano, L. 2008, MNRAS, 383, 1223

Merrifield, M. R. & Kuijken, K. 1994, ApJ, 432, 575

Minchev, I. & Famaey, B. 2010, ApJ, 722, 112

Minchev, I., Famaey, B., Combes, F., Di Matteo, P., Mouhcine, M., & Wozniak, H. 2011, A&A, 527, A147+

Moiseev, A. V. 2008, Astrophysical Bulletin, 63, 70

Mollenhoff, C. & Heidt, J. 2001, å, 368, 16

Noordermeer, E., van der Hulst, J. M., Sancisi, R., Swaters, R. A., & van Albada, T. S. 2005, A&A, 442, 137

Noordermeer, E. & van der Hulst, J. M. 2007, MNRAS, 376, 1480

Noordermeer, E., Merrifield, M. R., & Aragón-Salamanca, A. 2008, MNRAS, 388, 1381

Pohlen, M. & Trujillo, I. 2006, A&A, 454, 759

Press, W. H., Teukolsky, S. A., Vetterling, W. T., & Flannery, B. P. 1992, Numerical recipes in C. The art of scientific computing, ed. Press, W. H., Teukolsky, S. A., Vetterling, W. T., & Flannery, B. P.

Russell, D. G. 2002, ApJ, 565, 681

Salpeter, E. E. 1955, ApJ, 121, 161

Sánchez-Portal, M., Díaz, Á. I., Terlevich, R., Terlevich, E., Álvarez Álvarez, M., & Aretxaga, I. 2000, MNRAS, 312, 2

, Seigar, M. S. & James, P. A. 1998, MNRAS, 299, 672

Shapiro, K. L., Gerssen, J., & van der Marel, R. P. 2003, AJ, 126, 2707

Sil'chenko, O. K. & Afanasiev, V. L. 2000, A&A, 364, 479

Sil'chenko, O. K. & Moiseev, A. V. 2006, AJ, 131, 1336

Sotnikova, N. Y. & Rodionov, S. A. 2006, Astronomy Letters, 32, 649

Spitzer, Jr., L. 1942, ApJ, 95, 329

Toomre, A. 1964, ApJ, 139, 1217

van Albada, T. S., Kotanyi, C. G., & Schwarzschild, M. 1982, MNRAS, 198, 303

van der Marel, R. P. & Franx, M. 1993, ApJ, 407, 525

van Dokkum, P. G. 2001, PASP, 113, 1420

Verdes-Montenegro, L., Bosma, A., & Athanassoula, E. 1995, A&A, 300, 65